

# 1 Suitability of wheat straw semichemical pulp 2 for the fabrication of lignocellulosic 3 nanofibres and their application on 4 papermaking slurries

5 E. Espinosa<sup>[1]</sup>, Q. Tarrés<sup>[2]</sup>, M. Delgado-Aguilar<sup>[2]</sup>, I. González<sup>[2]</sup>, P. Mutje<sup>[2]</sup>, A.  
6 Rodríguez<sup>[1]</sup>

7  
8 *1) Chemical Engineering Department, Faculty of Science, University of Córdoba,*  
9 *Building Marie-Curie, Campus of Rabanales; 2) Group LEPAMAP, Department*  
10 *of Chemical Engineering, University of Girona, c/M. Aurèlia Campmany, n° 61,*  
11 *Girona 17071, Spain.*

12

## 13 Abstract

14 The present work studies the feasibility of wheat soda pulp as a raw material for the fabrication of  
15 cellulose nanofibres and their application as an additive in papermaking. Wheat straws were  
16 cooked under alkaline conditions and the resulting pulp was used as a raw material for the  
17 production of lignocellulosic nanofibres (LCNF). Nanofibres were fabricated by intense  
18 mechanical beating followed by high-pressure homogenization. The produced LCNF were  
19 characterized and applied to papermaking slurry based also on wheat straw soda pulp. Paper sheets  
20 made thereof were analysed for their physical and mechanical properties. The results indicated  
21 that paper strength was improved after addition of lignocellulose nanofibres (CNF), whereas  
22 density increased and porosity was reduced. These improvement in properties is significant  
23 (except the Tear Index) because they were achieved using LCNF with lower fibrillation degree  
24 compared to previous works where chemically pre-treated LCNF were used as reinforcement.

25 **Keywords:** *cellulose nanofibres, wheat straw pulp, paper, mechanical and*  
26 *physical properties*

27

## 28 Introduction

29 Sustainable development is a concept that is gaining more and more importance  
30 in our society, put into practice in all social aspects included industrial  
31 production. One of the pillars of sustainable development is the sustainable  
32 economy, which relies on integral utilization of natural resources. To achieve this  
33 goal it is necessary to valorise by-products and wastes produced in different  
34 activities such as agricultural or agro-industrial processes. Industrial activity has  
35 always relied on manufacturing products that meet the needs of customers within  
36 a market, but in recent years the environmental component has been incorporated  
37 into production since more and more society is aware and convinced of the  
38 necessity to consume products that have been obtained with environmentally  
39 friendly processes.

40 Europe produced over 96.5 million tons of paper and cardboard in the year 2010,  
41 where approximately a 17% was from non-wood raw materials (Confederation of  
42 European Paper Industries, CEPI). These non-wood raw materials are usually  
43 formed by residues from agriculture or agri-food industry; cellulosic fibres found

44 in this type of residues are useful for the fabrication of papers that have special  
45 characteristics due to its fibre morphology, composition and heterogeneity  
46 (García Hortal 2007, González - García *et al.* 2010). From all of these alternative  
47 raw materials, cereal straws are the most important source; world production of  
48 wheat, corn, barley, oats and rapeseed reached 1742 million tons in 2009 (FAO).  
49 Considering that a kilogram of grain generates approximately one kilogram of  
50 residue in the form of straws (Rodríguez *et al.*, 2010), agriculture generates a  
51 huge amount of wastes each year. These residues are used today, in the best of  
52 cases and in small quantities, as organic compost and as cattle feed. However,  
53 most of this residue is simply burnt in the field causing air pollution and risk of  
54 fire. Moreover, if these residues are not removed they can originate pest problems  
55 in the fields.

56 It is also important to consider the environmental aspects of wheat crop; each  
57 wheat plant has an annual CO<sub>2</sub> absorption of 10.3 g CO<sub>2</sub> / plant. If a wheat crop  
58 field has a density of 125 plants/m<sup>2</sup> (Carvajal 2008) then a hectare of crop would  
59 have an absorption capacity of 12875 tons CO<sub>2</sub> / has. From this amount, 3.5 tons  
60 of C are assimilated; this C would return to the atmosphere as CO<sub>2</sub> if plants are  
61 burnt. Therefore, integral use of this agricultural residue has not only economic  
62 advantages by enhancing what so far is a residue, but it has also direct  
63 environmental effects.

64 The use of cellulose nanofibres (CNF) as an additive for papermaking slurries has  
65 gathered increasing interest during the last years. Several recent publications  
66 confirm the improvement of paper's strength after addition of CNF as a bulk  
67 additive (Brodin *et al.* 2014, González *et al.* 2012, Taipale *et al.* 2010, Eriksen *et*  
68 *al.* 2008). The presence of CNF in the papermaking slurries boosts the formation  
69 of hydrogen bonds between fibres during paper formation, the main mechanism  
70 that dominates the increase of paper's strength. Besides, CNF promote reduction  
71 of porosity and increase of density in paper.

72 Fabrication of CNF consists mainly in disassembling the hierarchical structure of  
73 cellulose fibres by means of intense mechanical treatment. Usually, chemical  
74 (Saito *et al.* 2007, Wågberg *et al.* 2008, Besbes *et al.* 2011, González *et al.* 2014)  
75 or enzymatic (Janardhnan & Sain 2006, Pääkkö *et al.* 2007, Henriksson *et al.*  
76 2007) pre-treatments are applied to cellulose fibres in order to facilitate the  
77 mechanical treatment step and reduce energy consumption. However, the  
78 fabrication of CNF using only mechanical treatments has also been reported  
79 (Nogi *et al.* 2009, Spence *et al.* 2011, Ferrer *et al.* 2012, Afra *et al.* 2013). In fact,  
80 the first attempts to produce cellulose nanofibres were based only on mechanical  
81 treatments (Turbak *et al.* 1983). Most of these studies have been performed  
82 mainly on bleached chemical pulps from woody plants such as eucalyptus and  
83 pine. Other plant fibres have been also successfully used as a source of nanofibres  
84 after bleaching (Alila *et al.* 2013, Besbes *et al.* 2011). These authors reported that  
85 the properties of cellulose nanofibres from non-woody plants do not differ  
86 significantly from CNF of woody plants. Bleaching removes lignin,  
87 hemicelluloses and other polymer carbohydrates that naturally accompany  
88 cellulose fibres. The effect that these components have on the fabrication and  
89 properties of CNF was already studied by other authors (Spence *et al.* 2011,  
90 Ferrer *et al.* 2012, Chaker *et al.* 2013). Their results indicated that residual  
91 amounts of both lignin and hemicelluloses play a key role on the nanofibrillation

92 effectiveness. Basically, small amounts of lignin and high hemicelluloses content  
93 (25-30%) seem to have a beneficial effect during cellulose nanofibrillation by  
94 allowing obtaining high degrees of fibrillation. This means that cellulose fibres  
95 with such characteristics are potential candidates as raw materials for the  
96 production of CNF by using only mechanical disintegration.

97 In the present work, lingocellulosic nanofibres (LCNF) were fabricated from  
98 wheat straw soda pulps by applying only mechanical treatments via PFI-beating  
99 followed by high pressure homogenization and used as reinforcement for paper  
100 sheets fabricated from the same pulp. To our knowledge, this is the first time that  
101 LCNF are isolated from wheat residues using only mechanical treatment; the  
102 resulting nanofibres were then characterized and applied as a bulk additive in  
103 papermaking slurry of wheat pulp. Then papers sheets were fabricated and  
104 characterized for their physical and mechanical properties.

105

## 106 **Materials and methods**

### 107 **Materials**

108 Wheat straws were provided by Ecopapel S.L. from cooperatives of Écija, Sevilla,  
109 Spain. Because of the way in which these raw materials are harvested, it was  
110 necessary to first sift and perform a manual screening in order to separate  
111 undesirable elements such as stones, plastic bags, seeds, dust, wires, etc. Once  
112 these elements were separated, straws were dried at room temperature to constant  
113 moisture and stored in plastic bags for conservation. The content of  $\alpha$ -cellulose,  
114 holocellulose, lignin, ashes and ethanol extractable was determined according to  
115 TAPPI standards T-9m 54, T-203os61, T-222, T-211 and T-204, respectively.

### 116 **Methods**

#### 117 *Pulping and characterization of the pulps*

118 Wheat straws were pulped in a 15 L batch reactor at  $99 \pm 1^\circ\text{C}$  for 150min  
119 containing a 7% NaOH solution and heated by an outer jacket heater. The reactor  
120 contents were stirred by rotating the reaction vessel via a motor; the liquid/solid  
121 ratio was 10:1. After pulping, cooked material was dispersed in a pulp  
122 disintegrator at 1200 rpm for 30 min. The pulp was then passed through Sprout-  
123 Bauer beater and separated by sieving through a netting of 0.14 mm mesh size.  
124 The beating degree (Schopper-Riegler) of the resulting pulp was determined  
125 according to TAPPI T-227. The yield was determined by a gravimetric method  
126 after removing uncooked material ~~without cooking~~. Finally the content of  $\alpha$ -  
127 cellulose, lignin, holocellulose, ashes, ethanol extractable, Kappa number and  
128 viscosity were determined according to TAPPI standards T - 9m54, T-203 os61,  
129 T-222, T-211, T-204, T - 236cm 85 and T230-om-94, respectively.  
130 Morphological analysis and fines content was studied using a MorFI compact  
131 analyser (TechPap) controlled with a computer. The equipment analyses 1000 mL  
132 of a 1 wt% fibre suspension; about 10000 fibres were analysed by the software  
133 MorFI v. 8.2. The pulping and characterization process is resumed in Fig. 1.

134

135

**FIGURE 1 GOES HERE**

136 *LCNF production*

137 Lignocellulosic nanofibres were obtained by mechanical treatment. First, wheat  
138 soda pulp was beaten in a PFI beater (NPFI 02 Metrotec SA) according to ISO  
139 5264-2:2002 until achieving a drainage rate of 90 °SR. Then, a 1.5% aqueous  
140 suspension was prepared and passed through a PANDA PLUS 2000 (GEA NIRO)  
141 high pressure homogenizer following the next sequence: 4 times at 300 bars, 3  
142 times at 600 bars and 3 at 900 bars. This sequence was chosen to avoid clogging  
143 of the equipment in the first passes. During the process the temperature of the  
144 suspensions raised to 60-70° C. After this, the suspension was cooled down at  
145 room temperature and stored at 4° C. Fig. 2 resumes the fabrication and  
146 characterization process of LCNF used for the present study.

147

148 **FIGURE 2 GOES HERE**

149

150 *LCNF characterization*

151 The degree of polymerization (DP) of wheat soda fibres and LCNF was  
152 determined from intrinsic viscosity measurements, according to UNE 57-039-92.  
153 The viscosimetric average molecular weight was calculated from the equation:  $\eta$   
154 =  $K \cdot M^a$ , where  $\eta$  is the intrinsic viscosity,  $K = 2.28$  and  $a = 0.76$  (Henriksson *et*  
155 *al.* 2008). The water retention value (WRV) was measured by separating a  
156 determined volume of LCNF gel into two equal portions, which were then  
157 centrifuged in a Sigma Laborzentrifugen model 6K15 (7 cm of rotation radius) at  
158 2400 rpm for 30 minutes to eliminate non-bonded water. In order to retain the  
159 LCNF, a nitrocellulose membrane with a diameter pore of 0.22  $\mu\text{m}$  was used at  
160 the bottom of the centrifuge bottles. Once centrifuged, only the LCNF in contact  
161 with the membrane was removed, weighed and then dried at  $105 \pm 2^\circ \text{C}$  for 24 h in  
162 containers of previously measured weight. This methodology is partially based on  
163 TAPPI UM 256. The average WRV value was then calculated according to the  
164 next equation:

165

166 
$$WRV(\%) = \frac{w_w - w_d}{w_d} \times 100 \quad (1)$$

167

168  $W_w$  is the wet weight (g),  $W_d$  the dry weight (g). The carboxyl content (CC) of  
169 LCNF was calculated by conductometric titration. A dried sample (50–100 mg)  
170 was suspended in 15 ml of 0.01M HCl solution; this exchanges Na cations bound  
171 to the COOH group by H ions. After 10 min of magnetic stirring, the suspensions  
172 were titrated with 0.01M NaOH, adding 0.1 ml of NaOH to the suspension and  
173 then recording the conductivity in mS/cm; this process was repeated until  
174 observing a reduction, stabilization and increase in the conductivity. The CC is  
175 given by the following equation:

176

177 
$$CC = 162 (V_2 - V_1)c [(w - 36(V_2 - V_1)c]^{-1} \quad (2)$$

178

179 The results indicate the average in mmols of  $-\text{COOH}$  groups per gram of LCNF.  
180 The cationic demand of LCNF was also determined by means of a Mutek PCD 04  
181 particle charge detector, adapting the methodology described by Carrasco *et al.*

182 (1998). First, 0.04 g of LCNF (dried weight) was diluted in 1 L distilled water and  
 183 dispersed with a pulp disintegrator for 10 min at 3000 rpm. Afterwards, 10 mL  
 184 were taken and mixed with 25 mL of cationic polymer  
 185 polydiallyldimethylammonium chloride (poly-DADMAC) during 5 min with  
 186 magnetic stirring. After this, the mixture was centrifuged in a Sigma  
 187 Laborzentrifugen model 6 K 15 for 90 min at 4000 rpm. Then, 10 ml of the  
 188 supernatant were taken to the Müttek equipment. Anionic polymer (Pes-Na) was  
 189 then added to the sample drop by drop with a pipette until the equipment reached  
 190 0 mV. The volume of anionic polymer consumed was used to calculate the  
 191 cationic demand though the next equation:

$$192 \quad CD = \frac{(C_{PolyD} \cdot V_{PolyD}) - (V_{Pes-Na} \cdot C_{Pes-Na})}{W_{sample}} \quad (3)$$

194  
 195 Where CD is the cationic demand ( $\mu\text{eq/L}$ ),  $C_{PolyD}$  = cationic polymer  
 196 concentration (g/L),  $V_{PolyD}$  = used volume of cationic polymer (mL),  $C_{Pes-Na}$  =  
 197 anionic polymer concentration (g/L),  $V_{Pes-Na}$  = used volume of anionic polymer  
 198 (mL) and  $W_{sample}$  = sample's dry weight (g). The yield in nanofibrillation was  
 199 determined by centrifuging a 0.2 wt% suspension at 4500 rpm for 20 min in order  
 200 to isolate the nanofibrillated fraction (contained in the supernatant) from the non-  
 201 fibrillated and partially fibrillated one retained in the sediment fraction, which  
 202 was recovered, weighed and oven-dried at 90°C until constant weight. The yield  
 203 of nanofibrillation was then calculated from the next equation:

$$204 \quad \text{Yield\%} = \left(1 - \frac{\text{weight of dried sediment}}{\text{weight of diluted sample} \times \%Sc}\right) \times 100 \quad (4)$$

206  
 207 where %Sc represents the solid content of the diluted gel sample. Transmittance  
 208 measurements were performed on LCNF suspensions with 0.1% of solid content.  
 209 The sample was introduced in quartz cuvettes and the transmittance measured  
 210 with a UV-Vis Shimadzu spectrophotometer UV-160A set in the range between  
 211 400 and 800 nm. Distilled water was used as reference.

212 In addition, the effect of a 3wt% addition of the LCNF over a standard substrate  
 213 (bleached kraft hardwood pulp) was also studied. This pulp has 2098m of  
 214 breaking length and 15°SR. The methodology followed for this addition was the  
 215 same of incorporating LCNF into the wheat pulp suspension, as it is described in  
 216 the following section.

#### 217 *Determination of the energy consumption*

218 The energy consumption of the homogenizer during the production of LCNF was  
 219 carried out with an energy measuring equipment (Circutor CVM-C10), which  
 220 gives values of the energy consumption of the equipment or, what is the same, the  
 221 energy required from the electrical grid.

#### 222 *Incorporation of LCNF into the pulp suspension*

223 In the case of wheat suspensions with LCNF, they were added and mixed into the  
 224 semichemical wheat pulp slurry by means of a pulp disintegrator operating at  
 225 3000 rpm during 60 minutes and 1.5 % consistency using tap water (289  $\mu\text{S/cm}$ )  
 226 as background. This methodology has been used in previous works (Alcalá *et al.*

227 2013, González *et al.* 2012, 2013a, Delgado-Aguilar *et al.* 2014) and has proved  
228 to be effective in improving the dispersion of CNF in papermaking slurries. After  
229 this step, cationic starch and colloidal silica were added at corresponding doses of  
230 0.5 and 0.8 %, respectively, expressed on dry pulp. The application of these  
231 retention agents was done at gentle agitation of the suspension at 1% consistency  
232 for 20 min. This step becomes necessary in order to avoid the loss of LCNF  
233 during the dewatering process since filters at the bottom of the stock container in  
234 the Rapid-Köthen equipment are not able to retain nanometric material. The  
235 amount of LCNF added was calculated to obtain paper sheets with different  
236 percentages of LCNF (from 0 to 4 wt%). Paper sheets with an average basis  
237 weight of 75 g/m<sup>2</sup> were fabricated in a sheet former (ISP mod. 786FH) according  
238 to ISO standard 5269-2 and conditioned in a weather chamber at 25° C and 50%  
239 humidity for 48 h before mechanical tests were performed.

240

### 241 *Characterization of paper sheets*

242 Characterization of paper sheets obtained from the different fibrous suspensions  
243 was performed by determining first the basis weight (ISO 536) and thickness  
244 (ISO 534) of the sheet; density was calculated from the sheet's basis weight and  
245 the dimensions; Breaking length was calculated from tensile experiments  
246 performed in an Instron universal testing machine provided with 2.5 kN load cell.  
247 The testing conditions were set according to ISO standards 1924-1 and 1924-2.  
248 Tear index was determined in an Elmendorf Tearing Tester (mod. F53.98401  
249 Frank PTI) and assay conditions were set according to ISO standard 1974. Burst  
250 index tests were carried out in a burst tester (IDM mod. EM-50) and test  
251 conditions were set according to ISO standard 2758. Gurley porosity was  
252 determined in a Gurley porosimeter (Papelquímia) was used and testing  
253 conditions were set according to ISO standard 5636/5. Percentage of void volume  
254 (%), Scott bond (TAPPI T569). Percentage of void volume was calculated from  
255 the next equation:

256

$$257 \quad \text{Porosity (\%)} = 100 \cdot \left(1 - \frac{\rho_{\text{sample}}}{\rho_{\text{cellulose}}}\right) \quad (5)$$

258 where  $\rho_{\text{sample}}$  is the density of the paper sheet (calculated from basis weight,  
259 thickness and area) and  $\rho_{\text{cellulose}}$  is the density of cellulose, assumed to be 1.5  
260 gr/cm<sup>3</sup>.

261

### 262 *Scanning electron microscopy (SEM)*

263 The microscope was a Hitachi S-3000 variable pressure SEM (Hitachi High-  
264 Technologies Corporation, Minatoku, Tokyo, Japan). SEM surface images were  
265 acquired at 509 and 1,0009 magnifications, in secondary electron imaging mode.  
266 The acceleration voltage and working distance were 5 kV and 12 mm,  
267 respectively.

268

### 269 *Transmission electron microscopy (TEM)*

270 Transmission electron microscopy (TEM) was carried out with a ZEISS EM910  
271 TEM operating at 120 kV. Specimens for inspection by TEM were prepared by  
272 slowly evaporating one drop of the LCNF gel, at room temperature on a 400 mesh  
273 copper grid, coated by a carbon-supported film.



274

## 275 **Results and discussion**

### 276 **Wheat stalks characterization**

277 Wheat stalks presented the next composition: alcohol extractables (5.2%), ashes  
278 (7.72%),  $\alpha$ -cellulose (39.7%), hemicelluloses (30.6%) and lignin (17.7%). It can  
279 be said that the ash content is similar or even lower in comparison to similar  
280 agricultural residues such as corn (5.95%), oats (7%), rape (6.38%) and barley  
281 (9.49%), (Vargas *et al.* 2012). High values of ashes might give rise to problems of  
282 corrosion and fouling in the industrial plants. Lignin is a hydrophobic constituent,  
283 which if found in high proportions can hinder the refining process, since it  
284 inhibits the absorption of water from the pulp. However, a slight percentage of  
285 lignin, as in this case, gives to the pulp relatively high values of specific volume,  
286 dimensional stability and rigidity (García-Hortal 2007). Lignin content in wheat  
287 straws is very similar to those found in corn (18.2%), oats (16.6%), rape (17.2%)  
288 and barley (16.3%) (Vargas *et al.* 2012). The hemicellulose, in contrast to lignin,  
289 is very hydrophilic and this fact favors the swelling of fibres, increasing plasticity,  
290 flexibility and the ability to bind with other compounds, resulting in improvement  
291 of density, strength and physical properties of paper sheets (García-Hortal 2007).

292

### 293 **Pulp characterization**

294 Wheat soda pulp was characterized by determining the percentage of alcohol  
295 extractables, ashes,  $\alpha$ -cellulose, hemicellulose and lignin obtaining following  
296 values, respectively; 3.37%, 10.90%, 73.0%, 16.3 and 2.8%. Other characteristics  
297 were also determined such as yield, beating degree ( $^{\circ}$ SR), Kappa number and  
298 viscosity (mL/g) as reflected in table 1.

299

300 **TABLE 1 GOES HERE**

301

302 The yield obtained with the wheat straw soda pulp is around 70%, a high value  
303 within semi-chemical pulp and higher than yields achieved with other raw  
304 materials: corn (65.5%), oats (66.9%), rape (63.1%) and barley (65.6%), (Vargas  
305 *et al.* 2012). The drainage rate was relatively high compared to that of commercial  
306 chemical bleached pulps such as pine and eucalyptus. Higher  $^{\circ}$ SR is found in  
307 some chemithermomechanical pulps from other agricultural residues such as  
308 rapeseed (González *et al.*, 2013). An elevated Schopper-Riegler implies high  
309 bonding strength between the fibres (González *et al.*, 2012). The Kappa number is  
310 a measure of the delignification degree of the raw material. High values for this  
311 parameter imply that pulp is not adequate for bleaching process by its high cost.  
312 The value obtained for the wheat straw soda pulp (38.6) is the lowest of the  
313 different raw materials that have been compared (from 56.7 for the corn until  
314 115.1 for the rape). It must be pointed that the Kappa number found and the lignin  
315 content are not in agree. This is probably due to the accuracy in the gravimetric  
316 techniques that have been used for the chemical characterization. On the other

317 hand, the standard ISO 302:2004 provides a correlation between Kappa number  
318 and lignin content, in percentage (approximately 6.57). This constant is referred  
319 to wood pulps with values of Kappa numbers from 25 to 30. Applying this  
320 constant and taking the Kappa number determination as more accurate, the  
321 content of lignin would vary from 2.8% to 5.9%, being still a value quite low. The  
322 degree of polymerization (*DP*) calculated from intrinsic viscosity measurements  
323 was 1381.

324

325

## TABLE 2 GOES HERE

326

327 Table 2 presents the morphology of fibres after pulping. The detection limit for  
328 fines was set at 76 and 200  $\mu\text{m}$  in order to indicate the great amount of these  
329 particles present in the pulp. The presence of fines accounts for the high breaking  
330 length found in paper sheets fabricated from wheat soda pulp and the elevated  
331  $^{\circ}\text{SR}$  of its suspensions. As it is possible to see in table 2, the percentage of fines is  
332 higher when the detection limit is set at 200 $\mu\text{m}$ . Paper industry usually considers  
333 the fine elements those particles with lengths lower than 200 $\mu\text{m}$ . Setting the  
334 MorFi equipment at 200 $\mu\text{m}$ , Moreover, as shown later, the percentage of fines in  
335 the pulp plays an important role in the rate of increase of breaking length in  
336 LCNF-reinforced papers.

337

## 338 LCNF characterization

339 Characterization of LCNF is important since it helps to understand the  
340 mechanisms that rule the reinforcing effect that they have on papermaking  
341 slurries. Table 3 shows the characterization of the nanofibres used in this work.  
342 The PFI beating pre-treatment allows a greater capacity of hydration and swelling  
343 of fibres, thus facilitating the passing of the pulp suspension through the  
344 homogenizer.

345

346

## TABLE 3 GOES HERE

347

348 The LCNF of wheat straw have a nanofibrillation yield of 55.6%. This is a  
349 comparatively moderate result in contrast to NFC fabricated after TEMPO-  
350 oxidized fibres from bleached chemical pulps reported in the bibliography where  
351 nanofibrillation yield reaches over 95% (González *et al.* 2012, Delgado-Aguilar *et al.* 2014). These differences are a direct consequence of the type of pre-treatment  
352 applied on the pulp: in CNF fabricated from TEMPO-oxidized fibres, the  
353 formation of negatively-charged carboxyl groups in the C6 of the cellulose chain  
354 introduces repulsion forces between the fibres which promote water income, fibre  
355 swelling and hydration (Saito *et al.* 2007). This facilitates the disassembling of  
356 the fibre structure during the mechanical treatment.

358 Another important factor that determines the suitability of CNF production is the  
359 content of lignin and hemicelluloses. In general, the presence of these components



360 along with other heteropolysaccharides seems to ease the mechanical  
361 individualization of microfibrils; it has been inferred that hemicelluloses attached  
362 to microfibrils by hydrogen bonds form a physical barrier among them that  
363 inhibits the formation of microfibrils aggregates (Chaker *et al.* 2013). The same  
364 author concluded that, in the case of non-woody plants, a hemicellulose content of  
365 25% decisively stimulates high fibrillation. In the case of lignin Ferrer *et al.*  
366 (2012) reported that residual amounts of lignin promote fibrillation by stabilizing  
367 the radicals formed during beating stages. Moreover, the amorphous nature of  
368 lignin and hemicelluloses also influences the fibrillation process (Solala *et al.*  
369 2011). Therefore, it is clear that a high hemicellulose content and low amount of  
370 residual lignin make the wheat soda pulp a good candidate for LCNF production  
371 through solely mechanical treatment.

372

373

### FIGURE 3 GOES HERE

374

375 Transmittance is another method to indirectly measure the fibrillation degree of a  
376 LCNF suspension. The presence of cellulose fibres in the aqueous suspension  
377 leads to light scattering due to the differences in the refractive index between  
378 cellulose and water (1.5 and 1.3 respectively). Since the amount of scattered light  
379 is in relation to the particle size when Mie scattering is considered, then high  
380 transmittance values indicate that the suspended material has extensive fibrillation.  
381 Transmittance spectra from TEMPO-oxidized CNF are reported to be close to  
382 100% (Saito *et al.* 2007, Alila *et al.* 2013, Besbes *et al.* 2013, González *et al.*  
383 2014), indicating a very high fibrillation degree. In the case of LCNF from wheat  
384 pulp, the transmittance (Fig. 3) can be considered as comparatively moderate  
385 since no chemical pre-treatment was applied. Moreover, LCNF contain lignin  
386 which also causes light deflection. In the same way, the cationic demand is  
387 considerably lower than that obtained by TEMPO-catalyzed oxidation (González  
388 *et al.* 2014) as expected. Cationic demand serves also as an indirect indicator of  
389 the specific surface area of LCNF. Further mechanical treatment would lead to a  
390 slight increase in cationic demand. A possible mechanism of interaction between  
391 the cationic polymer (poly-DADMAC) an LCNF surface is reflected in Fig. 4.

392

393

### FIGURE 4 GOES HERE

394

395 This drawing tries to show the two possible mechanisms (Rouger and Mutjé,  
396 1984, Carrasco *et al.* 1996): i) ionic interaction between the cationic polymer and  
397 the carboxylic groups on the cellulose surface, and ii) surface interactions due to  
398 London-Van Der Waals forces. If both mechanisms are assumed to occur at the  
399 same time and that poly-DADMAC forms a single layer, then by estimating the  
400 specific surface area of a single poly-DADMAC ( $\sigma_{DADMAC}$ ) molecule, it would be  
401 then possible to theoretically calculate the specific surface area of LCNF ( $\sigma_{LCNF}$ ).  
402 Considering the atomic distances and angles between the atoms of a poly-  
403 DADMAC monomer and that the molecule adopts an elliptical structure then the

404 surface of the poly-DADMAC monomer could be calculated through the next  
405 equation:

$$406 \quad \sigma_{DADMAC} = \pi \cdot d \cdot l \quad 1)$$

407 where,  $\sigma_{DADMAC}$  is the monomer's area,  $d$  and  $l$  the diameter and length of the  
408 monomer's molecule, calculated to be 0.528 nm and 0.488 nm respectively. This  
409 makes 0.809 nm<sup>2</sup> for a single monomer molecule. Since the average degree of  
410 polymerization of poly-DADMAC is 662, the surface area of the polymer is the  
411 surface area of the monomer multiplied by degree of polymerization ( $DP$ ). This  
412 yields 535.56 nm<sup>2</sup> for a poly-DADMAC molecule. To calculate the specific  
413 surface area of a poly-DADMAC mol, the Avogadro constant is then applied:

$$414 \quad \sigma_{DADMAC} = 535.56 \text{ nm}^2 \cdot 6.02 \cdot 10^{23} = 3224 \cdot 10^{23} \text{ nm}^2/\text{mol} \quad 2)$$

415 Then,  $\sigma_{dadmac}$  is converted from nm<sup>2</sup>/mol to nm<sup>2</sup>/μeq by the next equation:

$$416 \quad \sigma_{DADMAC} = \frac{3224 \cdot 10^{23} \text{ nm}^2}{662 \cdot 10^6 \mu\text{eq}} = 4.87 \cdot 10^{17} \text{ nm}^2/\mu\text{eq} \quad 3)$$

417 Considering the stoichiometric relationship between hydroxyl and carboxyl  
418 groups with poly-DADMAC and applying the next relationship:

$$419 \quad \sigma_{LCNF} = (CD - CC) \cdot \sigma_{DADMAC} \quad 4)$$

420 where  $\sigma_{LCNF}$  is the specific surface area of one gram of LCNF, CD the cationic  
421 demand and CC the carboxyl content of the sample, then 75.77 m<sup>2</sup>/g was  
422 obtained. Finally, it is possible to calculate from this value the average diameter  
423 of a single LCNF fibre ( $d_{CNF}$ ), considering a cylindrical geometry:

$$424 \quad d_{CNF} = \frac{4}{75.77 \text{ m}^2/\text{g} \cdot 1600 \cdot 10^3 \text{ g}/\text{m}^3} \quad 5)$$

$$425 \quad d_{CNF} = 32.99 \text{ nm}$$

426 The diameter calculations based on the poly-DADMAC surface adsorption on the  
427 LCNF, show a mean diameter of approximately 33 nm. The actual diameter of  
428 LCNF was assessed by TEM microphotography, as reflected in Fig. 5.

429

430

## FIGURE 5 GOES HERE

431

432 The images show a wide distribution of widths with an average diameter of 28  
433 nm. This value is not significantly different from 33 nm calculated by the method  
434 described above. Though this theoretical calculation is based on a series of  
435 assumptions, it allows having an approximate idea of the evolution of  $\sigma_{LCNF}$  and  
436  $d_{CNF}$  in a simple, rapid manner. The TEM microphotography also shows that it is  
437 possible to obtain considerably nanofibrillated material by applying only  
438 mechanical forces on an unbleached, non-woody pulp.

439 The carboxyl content is considerably low when compared to values observed in  
440 TEMPO-oxidized CNF (Delgado-Aguilar *et al.* 2014) as expected. It is well  
441 known that intense fibrillation of cellulose fibres increases carboxylic content

442 which facilitates their dispersion in water, so it would be expected that further  
443 mechanical treatment would boost the carboxylic content. Regarding WRV, a  
444 result of 480% means that LCNF from wheat have 4.8 grams of water per gram of  
445 LCNF associated chemically. As a comparison, González *et al.*, (2014) obtained  
446 CNF of eucalyptus bleached pulp with a WRV of 1700%.

447 The viscosity of the LCNF suspension allowed calculating the degree of  
448 polymerization (1004.8). This indicates a reduction of 31% from the original *DP*  
449 of the soda pulp (1381) due to the mechanical forces applied for the preparation  
450 of LCNF. One of the main advantages of mechanical treatments for LCNF  
451 manufacture is that the loss in *DP* is not as intense as in LCNF prepared from  
452 some types of chemically modified fibres. The *DP* is directly linked to the  
453 intrinsic mechanical properties of the LCNF, as described in Henriksson *et al.*  
454 (2008).

455 The breaking length increase was assessed over the standard substrate described  
456 in the Materials and Methods chapter. This parameter helps to determine the  
457 effectiveness or performance that LCNF imparts on breaking length, as well as  
458 this parameter allows making reliable comparisons between different CNF. For  
459 instance, some published results showed that the addition of a 3wt% of CNF  
460 prepared by TEMPO oxidation (from bleached kraft hardwood pulp) at three  
461 different oxidation levels (3, 5 and 15mmols of hypochlorite) imparts an increase  
462 of about 97, 100 and 112% in breaking length, respectively (González 2014).

463 Using this parameter as part of the characterization of the produced CNF (or  
464 LCNF in the case of the present paper) allows knowing the effectiveness thereof.  
465 The main difference between the enhancement achieved between LCNF and CNF  
466 (TEMPO) is the diameter. While the average diameter of LCNF is 33nm, TEMPO  
467 oxidized cellulose nanofibers present diameters of between 3 and 10nm.

468 Since the production of LCNF for this study required intense mechanical  
469 treatment, an analysis of energy consumption was performed. Additionally, taking  
470 into account the amount of chemicals used for the production of TEMPO oxidized  
471 CNF and the passes through the homogenizer required to get those (Delgado-  
472 Aguilar *et al.* 2015), the production costs of this type of CNF (from bleached kraft  
473 hardwood pulp) were also calculated. The results are shown in table 4.

474

475

#### TABLE 4 GOES HERE

476

477 Regarding the case of LCNF, it is important to mention that this price does not  
478 take into account the energy consumption of soda pulping and the price of the  
479 chemicals used for such process. In this sense, in the case of TEMPO oxidized  
480 CNF, the price of obtaining the bleached pulp is also not included.

481 There are some methods reported elsewhere to determine the energy consumption  
482 of passing a suspension through the homogenizer (Ankerfors 2015, Naderi *et al.*  
483 2015). These methodologies are based on the energy balance between two data  
484 collection points (the surface of the inlet tank and after the pressure pump).  
485 Inasmuch as the energy losses of the internal and dynamical energy are quite  
486 difficult to measure, it has to be assumed that there are no changes, as well as in

487 the case of the sample heating due to friction in the chambers. Not just that, but  
488 the pump efficiency is also neglected, thus forcing to assume an efficiency of  
489 100%.

490 On the other hand, using the energy measurement equipment (Circutor CVM-  
491 C10), it is possible to determine the energy required, which is the same of the  
492 energy required from the electrical grid, becoming more reliable energy  
493 consumptions since it takes into account all the assumptions listed above. In fact,  
494 when assessing production costs, this is the energy that producers will be  
495 supposed to pay for.

496 As it is possible to see, the energy required for LCNF is higher than for CNF  
497 (TEMPO oxidized). This is mainly due to the effect of TEMPO oxidation, since  
498 the pretreatment is harder than in the case of LCNF and the energy required to  
499 nanofibrillate becomes lower.

500 Looking at the total production costs, it is possible to see that TEMPO CNF is  
501 about 70 times more expensive than LCNF. This difference is mainly due to  
502 chemicals costs. Nowadays, there is still missing a methodology to recover  
503 successfully TEMPO catalyst, which costs about 8,800€/kg. Looking at the costs  
504 breakdown of this type of CNF, it is possible to see that TEMPO represents about  
505 80% of the total cost.

#### 506 **Bulk application of LCNF on wheat soda pulp**

507 To evaluate the feasibility of wheat straws in the papermaking industry, paper  
508 sheets from wheat soda pulps were fabricated and added with different  
509 percentages of LCNF in combination with cationic starch and colloidal silica as  
510 retention agents. The first one, cationic starch, is added in order to ensure a good  
511 retention of the LCNF on paper. On the other hand, and due to the flocculation  
512 effect of cationic starch, colloidal silica is added in order to ensure a good paper  
513 formation. The physical properties of the manufactured paper sheets are shown in  
514 table 5.

515

#### 516 **TABLE 5 GOES HERE**

517

518 The results indicate that, under a constant grammage, paper's thickness decreases  
519 with growing contents of LCNF. Probably, nanofibres moving freely in fibres  
520 suspensions behave in a way similar to that of fines by reducing the meniscus  
521 radius that appears during dewatering of the papermaking suspension; this  
522 increases the pressure difference between the aqueous phase and the fibres  
523 surroundings, helping thus to draw the fibres closer together, compacting the  
524 paper sheet. Besides, nanofibres attached to the larger fibres' surface significantly  
525 increase the contact area between fibres which boost the formation of hydrogen  
526 bonds and establish permanent bonds among the fibres when they are brought into  
527 contact during the dewatering step. This also explains the increase in density  
528 higher LCNF contents. Papers with a 4 wt% of LCNF presented the highest  
529 density. Porosity calculated as the percentage of empty space is also reduced with  
530 the presence of LCNF. The decrease in porosity is also a consequence of the  
531 increase in paper's compactness. It is also expected that a part of the nanofibres

532 occupy the spaces between the larger fibres, forming a nanometer network that  
533 occupy the gaps between fibres. As a whole these mechanisms help to reduce the  
534 diameter and number of pores of the paper. The same trend is observed in the  
535 Gurley porosity, whose test time increases until a 685% versus paper sheets made  
536 of pulp without reinforcement. Test times develop linearly in relation to the  
537 amount of LCNF. In fact, the evolution of physical properties in paper sheets has  
538 a good correlation with the content of the LCNF as shown in Fig. 6.

539

540

**FIGURE 6 GOES HERE**

541

542 Table 6 summarizes the Schopper-Riegler and mechanical properties of LCNF-  
543 reinforced papers sheets. Neat wheat straw soda pulp has a high Schopper-Riegler  
544 in comparison to a typical bleached eucalyptus pulp (González *et al.* 2012).

545

546

**TABLE 6 GOES HERE**

547 An elevated °SR is consequence of the high percentage of fines found in wheat  
548 straw pulp in comparison to bleached chemical pulps; these fines increase the  
549 specific surface of the pulp and block the spaces between fibres where water  
550 drains, increasing the °SR. After addition of LCNF, the °SR increases due to the  
551 high water-holding capacity that LCNF in general show. The large specific  
552 surface area of LCNF promotes the formation of hydrogen bonds between the  
553 hydroxyl groups of cellulose and water. This causes that the LCNF retain a great  
554 quantity of water even at low concentrations, modifying the viscosity of the  
555 suspension and hampering dewatering. As the LCNF content rises, °SR  
556 significantly increases. The evolution of °SR shows a correlation with the amount  
557 of LCNF (Fig. 7).

558

559

**FIGURE 7 GOES HERE**

560

561 With regard to the mechanical properties of paper sheets made without LCNF, it  
562 is important to highlight that this fibre already has a breaking length suitable for  
563 the manufacture of certain types of paper. Fig. 7 shows the evolution of the  
564 breaking length according to the percentage of LCNF added; the results obtained  
565 are from paper sheets made with an isotropic former. It can be observed that  
566 breaking length experiences a linear increase up to a 28% with the addition of a  
567 3% of LCNF. Tensile strength of paper mainly depends on three factors: the  
568 number of links among fibres, the type of links and the intrinsic resistance of the  
569 fibre. The improvement observed in paper reinforced with LCNF is due to the  
570 boost in the number of hydrogen bonds between fibres promoted by the greater  
571 specific surface area of the LCNF. More than 3 wt% of LCNF did not bring about  
572 an improvement in breaking length probably because there is no more linkable  
573 area available. The burst index also increased up to 50% after the addition of 4%  
574 of LCNF. In contrast to the other physical properties, tear index showed its  
575 maximum value with 1% of LCNF, being this increase of a 7.1% versus initial

576 value. This is because in pulps with low degree of union between the fibres, the  
577 tear index increases when the fibre-to-fibre union improves, as it is the case with  
578 the addition of LCNF. However, when the degree of union between fibres is  
579 already high, as in the case of pulps reinforced with LCNF, tear index is  
580 determined by the strength and length of the fibres, so larger amounts of LCNF  
581 will not produce significant improvement of the tear index.

582

### 583 **Interactions between wheat fibres, fines and LCNF**

584 The rate of increase in breaking length after LCNF addition depends on the tensile  
585 strength of fibres and their morphological properties. This means that pulps and  
586 fibres with different morphology and tensile strength will increase their breaking  
587 length at different rates. Considering that the increase in the number of hydrogen  
588 bonds between fibres is the main mechanism of resistance of paper, it is expected  
589 that fibres with a low binding capacity show higher rate increase than those that  
590 are well linked. Therefore, it can be accepted that mechanical and recycled pulp  
591 show a more significant increase than, for example, beaten chemical pulps  
592 (Brodin *et al.* 2014). However, when LCNF were used to reinforce papermaking  
593 slurries from bleached eucalyptus pulp, breaking length improved from 2098 to  
594 3972 m, an increase of 89% after addition of 3 wt% of LCNF; this rate of increase  
595 is far superior than seen in paper sheets from wheat soda pulp with the same  
596 nanofibres content, as it has been explained before.

597

### 598 **FIGURE 8 GOES HERE**

599

600 In order to understand this difference in the rate of increase it is important to  
601 consider the role that the high content of fines may have in the interaction  
602 between wheat soda pulp and LCNF.

603

### 604 **FIGURE 9 GOES HERE**

605

606 During paper formation, the fines that freely float in the water interact with the  
607 LCNF in such a way that a part of the nanofibres forms links with the fines and  
608 not with the fibres. This would significantly reduce the reinforcing effect of  
609 nanofibres while the °SR would remain at high levels by the combined effect of  
610 fines and LCNF. Fig. 8 shows the proposed mechanism of interaction among  
611 fines, LCNF and fibres within the suspension. It is expected, therefore, that by  
612 removing fines before the addition of LCNF it could be possible to improve the  
613 linking ability of LCNF with fibres, which could ultimately lead to more  
614 significant increases in paper's strength. According to this reasoning, paper sheets  
615 with 3 wt% of LCNF were fabricated from wheat soda pulp without fines.  
616 Mechanical tests indicated an improvement in breaking length from originally  
617 5713m (wheat semichemical pulp with 13.9% of fine content) to 7609 m. This  
618 result clearly shows that the presence of fines limits the reinforcing effect of

619 LCNF. The interaction between LCNF and fibres within the paper sheet structure  
620 has been observed through FE-SEM (Fig. 9). The images indicate that the LCNF  
621 are distributed either filling the gaps between (right picture) fibres or partially  
622 covering them (left picture). Both types of distribution increase the amount of  
623 hydrogen bonds between fibres, accounting for the significant increase in  
624 mechanical properties even at low LCNF content.

625

## 626 **Conclusions**

627 In this work, the feasibility of wheat straw as a raw material to produce  
628 lignocellulose nanofibres and their application as papermaking additive was  
629 studied. This pulp was chosen due to its relatively low residual lignin content and  
630 high amount of hemicelluloses. LCNF were prepared using mechanical pre-  
631 treatment via PFI beater followed by high-pressure homogenization. The  
632 nanofibrillation degree was moderate in comparison to CNF prepared from  
633 TEMPO-oxidized fibres and the characterization confirmed the lower content of  
634 nanosized material. In addition, it has been demonstrated that TEMPO oxidized  
635 CNF are 70 times more expensive than LCNF from wheat semichemical pulp.  
636 The use of LCNF on papermaking slurry based on wheat soda pulp induced an  
637 improvement in breaking length and burst index in relation to unreinforced paper,  
638 whereas tear index remained almost constant. Besides, paper sheets became  
639 thinner as more LCNF was added, leading to an increase in density and a  
640 reduction in porosity. It was also demonstrated that the presence of fines can  
641 sensibly hinder the rate of increase in paper's mechanical properties. By removing  
642 fines, the rate of increase was significantly improved in comparison with fine-  
643 containing pulps.

644

## 645 **Acknowledgments**

646 The authors are grateful to Spain's DGICYT, MICINN for funding this research  
647 within the framework of the Projects CTQ2013-46804-C2-2-R.

648

## 649 **References**

650 Afra E, Yousefi H, Hadilam MH, Nishino T. (2013) Comparative effect of  
651 mechanical beating and nanofibrillation on paper properties made from bagasse  
652 and softwood pulps. *Carbohydr Polym*, 97, 725-730.

653 Alila S, Besbes I, Rei Vilar M, Mutjé P, Boufi S. (2013) Non-woody plants as  
654 raw materials for production of microfibrillated cellulose (MFC): A comparative  
655 study. *Ind Crop Prod*, (41), 250-259.

656 Ankerfors, M. (2015). Microfibrillated cellulose: Energy-efficient preparation  
657 techniques and applications in paper.



- 658 Besbes I, Rei Vilar M, Boufi S. (2011) Nanofibrillated cellulose from Alfa,  
659 Eucalyptus and Pine fibres: Preparation, characteristics and reinforcing potential.  
660 *Carbohyd Polym*, 86, 1198-1206.
- 661 Brodin FW, Gregersen ØW, Syverud K (2014) Cellulose nanofibrils: Challenges  
662 and possibilities as paper additive or coating material. *Nor Pulp Pap Res J*, 29 (1),  
663 156-166.
- 664 Carrasco, F., Mutje, P., & Pelach, M. A. (1996). Refining of bleached cellulosic  
665 pulps: Characterization by application of the colloidal titration technique. *Wood*  
666 *Sci Technol*, 30(4), 227-236.
- 667 Carrasco, F., Mutjé, P., & Pelach, M. A. (1998). Control of retention in paper-  
668 making by colloid titration and zeta potential techniques. *Wood Sci*  
669 *Technol*, 32(2), 145-155.
- 670 Carvajal, M., Mota, C., Alcaraz-López C., Iglesias M. and Martínez Ballesta M.C.  
671 (2008) Investigación sobre la absorción de CO<sub>2</sub> por los cultivos más  
672 representativos. Accessed November 2014.
- 673 Chaker A, Alila S, Mutjé P, Rei Vilar M, Boufi S (2013) Key role of the  
674 hemicelluloses content and the cell morphology on the nanofibrillation  
675 effectiveness of cellulose pulp. *Cellulose*, 20, 2863-2875.
- 676 Delgado-Aguilar, M., González, I., Pelach, M. A., De La Fuente, E., Negro, C., &  
677 Mutjé, P. Improvement of deinked old newspaper/old magazine pulp suspensions  
678 by means of nanofibrillated cellulose addition. *Cellulose*, 22 (1), 789-802.
- 679 Eriksen Ø, Syverud K, Gregersen Ø (2008) The use of microfibrillated cellulose  
680 produced from kraft pulp as strength enhancer in TMP paper. *Nor Pulp Pap Res J*,  
681 23(3), 299-304.
- 682 Ferrer A, Quintana E, Filpponen I, Solala I, Vidal T, Rodríguez A, Laine J, Rojas  
683 OJ. (2012) Effect of residual lignin and heteropolysaccharaides in the  
684 nanofibrillar cellulose and nanopaper from wood fibers. *Cellulose*, 19, 2179-2193.
- 685 García Hortal, J.A. (2007) "Fibras papeleras," Universidad Politécnica Cataluña.
- 686 González, I. (2014). Production and Characterization of Nanofibrillated Cellulose  
687 from Eucalyptus Fibres and its Application on Papermaking. Doctoral Thesis.  
688 Universitat de Girona.
- 689 González I, Boufi S, Pelach M, Alcalá M, Vilaseca F, Mutjé P. (2012)  
690 Nanofibrillated cellulose as paper additive in eucalyptus pulps. *BioResources*, 7  
691 (4), 5167-5180.
- 692 González I, Alcalá M, Arbat G, Vilaseca F, Mutjé P (2013) Suitability of rapeseed  
693 chemithermomechanical pulp as raw material in papermaking. *BioResources*,  
694 8(2), 1697-1708.
- 695 González I, Alcalá M, Chinga-Carrasco G, Vilaseca F, Boufi S, Mutjé P. (2014)  
696 From paper to nanopaper: evolution of mechanical and physical properties.  
697 *Cellulose* 21 (4), 2599-2609.

- 698 González–García S, Moreira MT, Artal G, Maldonado Ll, Feijoo G (2010)  
699 Environmental impact assesment of non-wood based pulp production by soda-  
700 anthraquinone pulping process. *J. Clean Prod*, 18(2), 137-145.
- 701 Henriksson M, Henriksson G, Berglund LA, Lindström T (2007) An  
702 environmentally friendly method for enzyme-assisted preparation of  
703 microfibrillated cellulose (MFC) nanofibers. *Eur Polym J*, 43, 3434-3441.
- 704 Henriksson M, Berglund LA, Isaksson P, Lindström T, Nishino T (2008)  
705 Cellulose Nanopaper Structures of High Toughness. *Biomacromolecules* 9, 1579-  
706 1585.
- 707 Janardhnan S, Sain MM, (2006) Isolation of cellulose microfibrils – An  
708 enzymatic approach. *BioResources*, 1(2), 176-188.
- 709 Naderi, A., Lindström, T., & Sundström, J. (2015). Repeated homogenization, a  
710 route for decreasing the energy consumption in the manufacturing process of  
711 carboxymethylated nanofibrillated cellulose?. *Cellulose*, 22(2), 1147-1157.
- 712 Nogi M, Iwamoto S, Nakagaito AN, Yano H (2009) Optically transparent  
713 nanofibre paper. *Adv Mater*, 21, 1595-1598.
- 714 Pääkkö M, Ankerfors M, Kosonen H, Nykänen A, Ahola S, Österberg M,  
715 Ruokolainen J, Laine J, Larsson PT, Ikkala O, Lindström T (2007). Enzymatic  
716 hydrolysis combined with mechanical shearing and high-pressure homogenization  
717 for nanoscale cellulose fibrils and strong gels. *Biomacromolecules*, 8, 1934-1941.
- 718 Rodríguez A, Sánchez R, Requejo A, Ferrer A. (2010) Feasibility of rice straw as  
719 a raw material for the production of soda cellulose pulp. *J. Clean Prod*, 18, 1084-  
720 1091.
- 721 Rouger, J., & Mutjé, P. (1984). Correlation between the cellulose fibres beating  
722 and the fixation of a soluble cationic polymer. *Brit Polym J*, 16(2), 83-86.
- 723 Saito T, Kimura S, Nishiyama Y, Isogai A (2007) Cellulose nanofibres prepared  
724 by TEMPO-mediated oxidation of native cellulose. *Biomacromolecules*, 8, 2485-  
725 2491.
- 726 Solala I, Volperts A, Andersone A, Dizhbite T, Mironova-Ulmane N, Vehniäinen  
727 A, Pere J, Vuorinen T (2011) Mechanoradical formation and its effects on birch  
728 kraft pulp during the preparation of nanofibrillated cellulose with Masuko  
729 refining. *Holzforschung*, 66, 477-483.
- 730 Spence K, Venditti RA, Rojas OJ, Habibi Y, Pawlak JJ (2011) A comparative  
731 study of energy consumption and physical properties of microfibrillated cellulose  
732 produced by different processing methods. *Cellulose*, 18, 1097-1111.
- 733 Taipale T, Österberg M, Nykänen A, Ruokolainen J, Laine J (2010) Effect of  
734 microfibrillated cellulose and fines on the drainage of kraft pulp suspension and  
735 paper strength. *Cellulose* 17, 1005-1020.
- 736 Turbak A, Snyder F, Sandberg K (1983) Microfibrillated cellulose: a new  
737 cellulose product: properties, uses, and commercial potential. *J Appl Polym Sci*  
738 *Appl Polym Symp* 37:815–827.

- 739 Vargas F, González Z, Sánchez R, Jiménez L, Rodríguez A (2012). Straw pulps  
740 for packaging. *BioResources* 7(3), 4161-4170.
- 741 Yoo S, Hsieh JS (2010) Enzyme-assisted preparation of fibrillated cellulose fibers  
742 and its effect on physical and mechanical properties of paper sheet composites.  
743 *Ind Eng Chem Res*, 49, 2161-2168.
- 744 Wågberg L, Decher G, Norgren M, Lindström T, Ankerfors M, Axnäs K (2008)  
745 The build-up of polyelectrolyte multilayers of microfibrillated cellulose and  
746 cationic polyelectrolytes. *Langmuir*, 24, 784-795.
- 747 [www.cepi.org](http://www.cepi.org) , key statics 2010. Accessed November 2014
- 748 [www.fao.org](http://www.fao.org) , Accessed November 2014

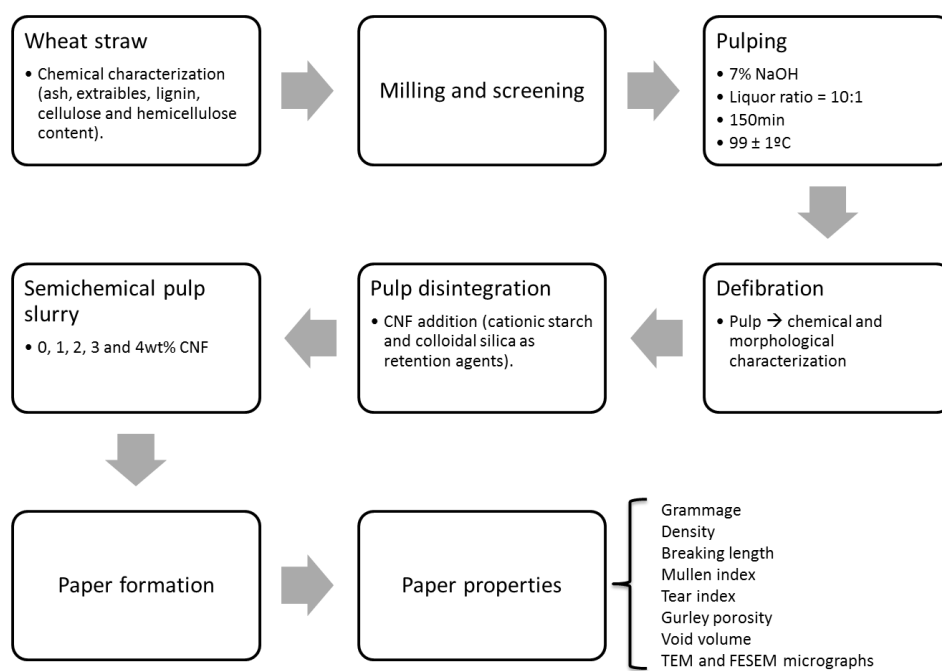


**Fig. 1.** Flow chart of the whole wheat soda pulp fabrication process and characterization.

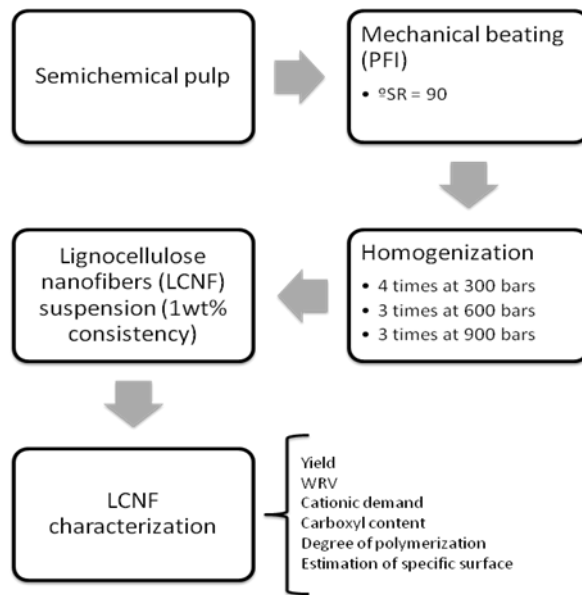


**Fig. 2.** Flow chart of the fabrication and characterization of LCNF

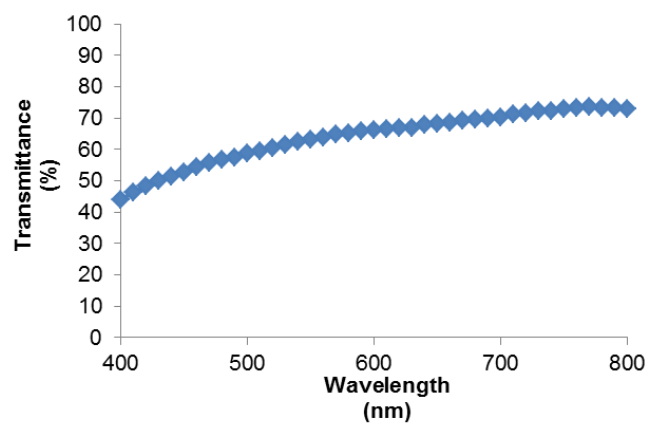


**Fig. 3.** Transmittance of the suspension of CNF in the range of the visible light spectrum

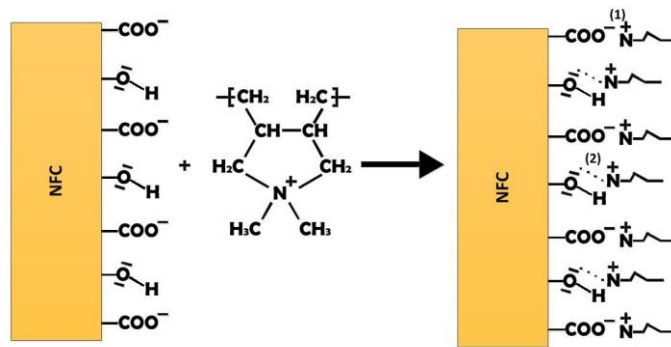


**Fig. 4.** Proposed mechanisms of interaction between LCNF and poly-DADMAC.



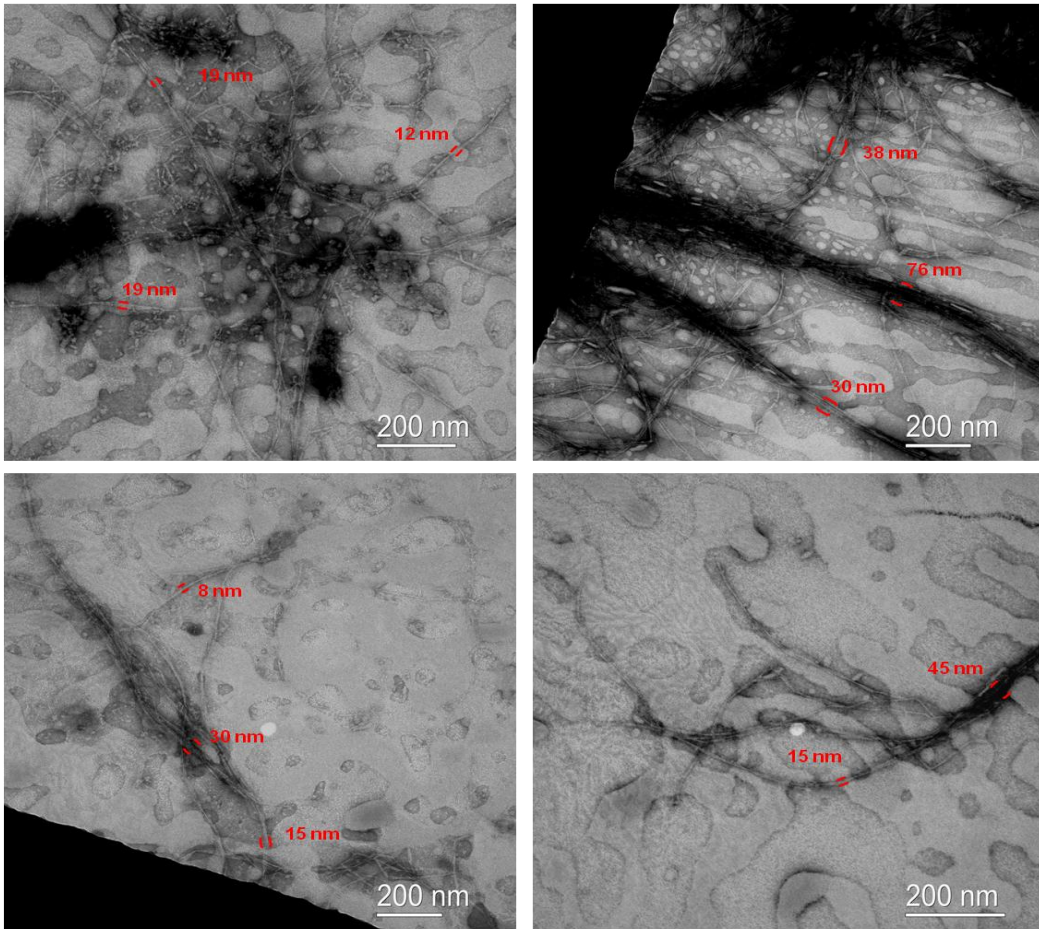


**Fig. 5.** TEM images of LCNF indicating the diameter of some of the nanofibres.

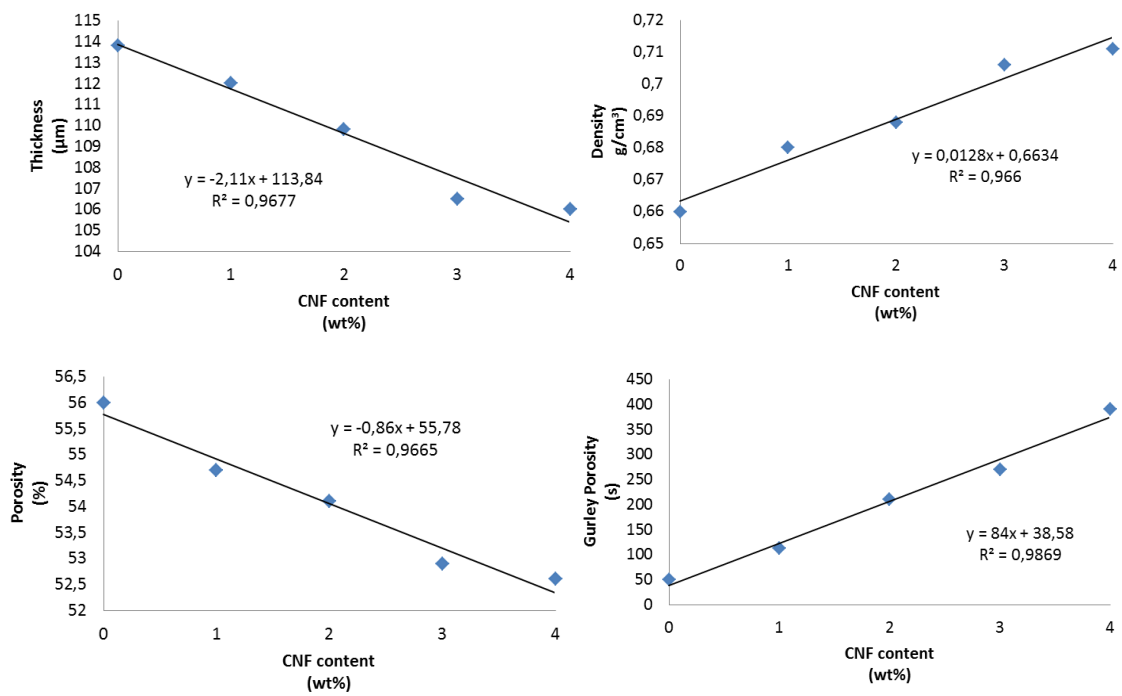


**Figure 6.** Evolution of the physical properties of papers based on the contents of CNF.

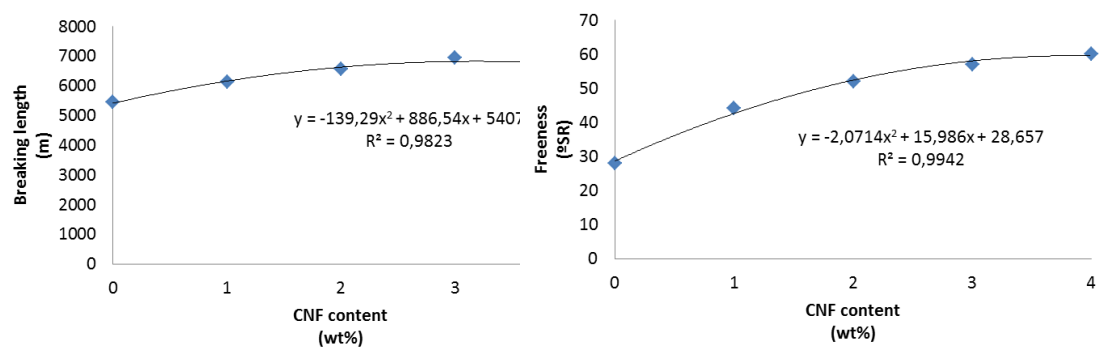


**Fig. 7.** Evolution of the breaking length (left) and Schopper-Riegler (right) of wheat straw pulps in relation with the CNF content

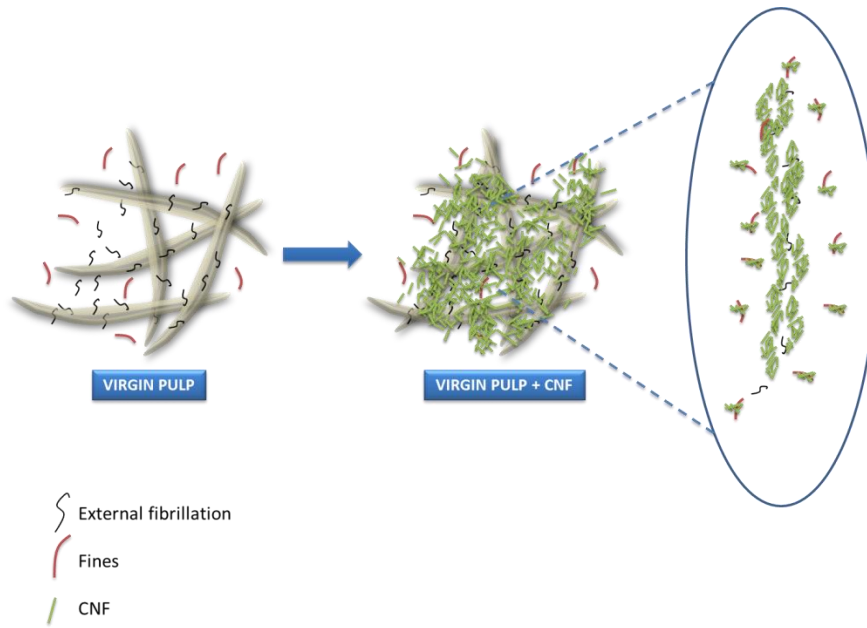


**Figure 8.** Proposed mechanism of interaction between fines, CNF and fibres.

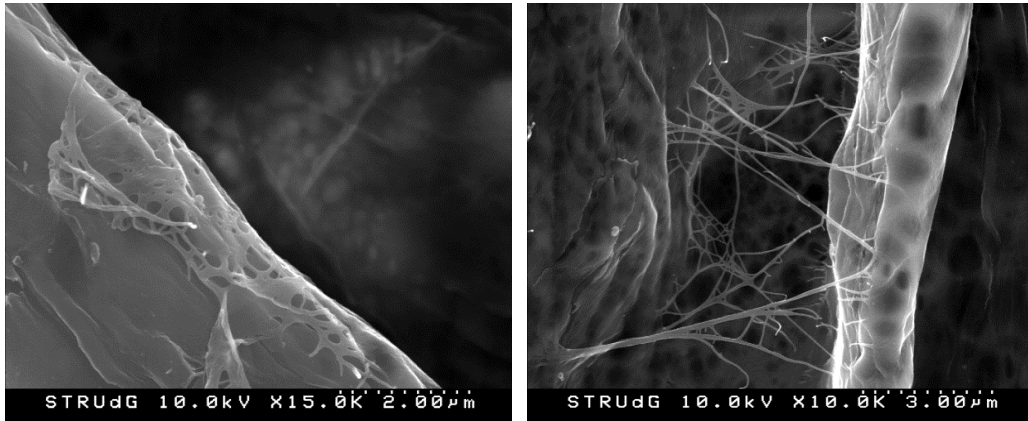


**Fig. 9.** Interaction between CNF and fibres. Left) LCNF covering the surface of a fibre; right) LCNF occupying the gaps between fibres.

**Table 1.** Wheat soda pulp properties.

<b>Yield</b> (%)	<b>°SR</b>	<b>Kappa number</b>	<b>Viscosity</b> (mL/g)	<b>DP</b>
70	51	38.6	536	1381

**Table 2.** Morphology of the wheat soda pulp fibres in relation to the fines detection limit set during the experiment.

<b>Fines detection limit</b>	<b>Length arithmetic</b>	<b>Length weighted in length</b>	<b>Width</b>	<b>Fines</b>	<b>Breaking length</b>
( $\mu\text{m}$ )	( $\mu\text{m}$ )	( $\mu\text{m}$ )	( $\mu\text{m}$ )	(% in length)	(m)
76	502	730	20.1	26.9	5435
200	510	742	20.1	47.6	5435



**Table 3.** Characterization of the LCNF

<b>Yield</b> (%)	<b>Transmittance</b> (%)	<b>Cationic demand</b> ( $\mu\text{eq}\cdot\text{g}/\text{g}$ )	<b>Carboxyl content</b> ( $\mu\text{eq}\cdot\text{g}/\text{g}$ )	<b>WRV</b> (%)	<b>Viscosity</b> (mL/g)	<b>DP</b>	<b>Breaking length increase</b> (%)
55.6	<75	230	<74.4	480.3	436	1004.8	89.31

**Table 4.** Energy consumption for the production of cellulose nanofibres.

Type of CNF	Chemicals				Pressure (bar)	Number of passes	Energy consumption (kW·h/kg)	Price* (€/kg)
	TEMPO (€/kg CNF)	NaBr (€/kg CNF)	NaOH (€/kg CNF)	NaClO (€/kg CNF)				
Wheat LCNF					300	4	14,22	1,14
					600	3	11,00	0,88
					900	3	6,66	0,53
TEMPO CNF (5mmols)	140,70	10,67	20,13	1,79	600	3	29,2	2,34

**Wheat LCNF: Total Price\* (€/kg) = 2,55**

**TEMPO CNF: Total Price\* (€/kg) = 175,63**

\* Total price calculated at a price of 0,08€/kW · h

**Table 5.** Physical properties of the paper sheets made with different percentages of LCNF.

<b>CNF content</b> (wt%)	<b>Grammage</b> (m <sup>2</sup> /g)	<b>Thickness</b> ( $\mu$ m)	<b><math>\rho_{\text{paper}}</math></b> (g/cm <sup>3</sup> )	<b>Porosity</b> (%)	<b>Gurley porosity</b> (seconds)
<b>Wheat + 0% CNF</b>	75.10 $\pm$	113.8 $\pm$ 0.1	0.660 $\pm$	56 $\pm$ 0.3	49.8 $\pm$ 0.2
<b>Wheat + 1% CNF</b>	76.15 $\pm$	112 $\pm$ 0.5	0.680 $\pm$	54.7 $\pm$ 0.6	112.3 $\pm$ 0.4
<b>Wheat + 2% CNF</b>	75.50 $\pm$	109.8 $\pm$ 0.6	0.688 $\pm$	54.1 $\pm$ 0.4	209.9 $\pm$ 0.4
<b>Wheat + 3% CNF</b>	75.25 $\pm$	106.5 $\pm$ 0.5	0.706 $\pm$	52.9 $\pm$ 0.7	269.9 $\pm$ 0.7
<b>Wheat + 4% CNF</b>	75.40 $\pm$	106 $\pm$ 0.4	0.711 $\pm$	52.6 $\pm$ 0.3	391 $\pm$ 0.6

**Table 6.** Drainage and mechanical properties of the paper sheets with different percentages of LCNF.

<b>CNF content</b> (wt%)	<b>°SR</b>	<b>Breaking length</b> (m)	<b>Burst index</b> (Kpa·m <sup>2</sup> /g)	<b>Tear index</b> (mN·m <sup>2</sup> /g)
<b>Wheat + 0% CNF</b>	28	5435±115	2.38±0.12	4.2±0.01
<b>Wheat + 1% CNF</b>	44	6121±87	2.98±0.05	4.5±0.03
<b>Wheat + 2% CNF</b>	52	6555±102	3.16±0.09	4.4±0.02
<b>Wheat + 3% CNF</b>	57	6937±91	3.39±0.10	3.9±0.07
<b>Wheat + 4% CNF</b>	60	6674±77	3.65±0.11	4.3±0.04